Frontiers of Information Technology & Electronic Engineering
www.jzus.zju.edu.cn; engineering.cae.cn; www.springerlink.com
ISSN 2095-9184 (print); ISSN 2095-9230 (online)
E-mail: jzus@zju.edu.cn

A novel frequency-protection interval adjustment method based on Doppler frequency offset pre-compensation for space-based Internet of Things*

Qingquan LIU†1, Lihu CHEN†‡1, Songting LI[1], Yiran XIANG[1], Baokang ZHAO[2]

[1]*College of Aerospace Science and Engineering, National University of Defense Technology, Changsha 410073, China*

[2]*College of Computer Science and Technology, National University of Defense Technology, Changsha 410073, China*

†E-mail: liuqq_wy2022@163.com; chenlihu05@nudt.edu.cn

Received Jan. 14, 2024; Revision accepted May 16, 2024; Crosschecked May 29, 2025

Abstract: To meet the access demands of massive terminal users, the space-based Internet of Things (IoT) requires sufficient frequency resources for allocation. However, the frequency resources that are currently available have already been allocated to a great extent. Furthermore, the utilization rate of the allocated frequency resources is low. To support massive user access under restricted frequency resources, this work proposes a scheme based on Doppler frequency offset (DFO) pre-compensation to enhance spectrum utilization efficiency. By calculating the relative motion between the satellite and the transmitting terminal, combined with the length and transmission rate of the message, the optimal compensation value of the Doppler frequency deviation is determined. The frequency-protection interval is reduced. Simulation results show that the pre-compensation method can expand the user access volume by 90–400 times. Properly selecting the number of message splits and transmission rate to perform DFO pre-compensation calculations can increase user access by an additional 45% or more. This method improves the spectrum utilization efficiency and provides a solution to the challenge of access by a large number of users.

Key words: Protection interval; Spectrum utilization; Doppler frequency offset pre-compensation; Massive user access

https://doi.org/10.1631/FITEE.2400033 **CLC number:** TN927

1 Introduction

Space-based Internet of Things (IoT) is an effective compensation and extension of the ground-based IoT. It utilizes various types of space-based platforms to realize the acquisition, processing, transmission, and application of IoT information. It has become a fundamental technical means for building the interconnection of all things and for ubiquitous sensing. The space-based IoT system has the advantages of being able to realize global coverage, all-weather operation, and strong stability. It has been widely used in logistics monitoring, transportation, environmental protection, hydrological monitoring, and other fields (Chen et al., 2022; Yang H et al., 2022; Li K et al., 2023; Yu TK et al., 2024a). However, the frequency resources that need to be relied upon for space-based IoT are currently facing two prominent problems. One is the scarcity of the remaining frequency resources that can be used for division; the Ku frequency band, as the "golden frequency band" for low-orbit satellite communication, has almost been completely allocated. The other is that the divided frequency resources have not been used aptly or the utilization rate is low, and most of the divided frequency resources are in an idle state (Tan

‡ Corresponding author

* Project supported by the Proximity Space Science, Technology and Industry Guidance Fund (No. LKJJ-2023022-01)

ORCID: Qingquan LIU, https://orcid.org/0009-0002-1761-5602; Lihu CHEN, https://orcid.org/0000-0002-9160-1981

© Zhejiang University Press 2025

et al., 2018). Yang Y (2019) listed that the average spectrum utilization rate of different frequency bands <3 GHz provided by the shared spectrum to the National Science Foundation is only 5.2% (FCC, 2002). About 31.25% of the total number of sub-band carriers in the IEEE802.15.3c standard are blank carriers (Ge et al., 2016). Meanwhile, the Global System for Mobile Communications Association predicted that the global scale of IoT connections in 2025 will reach 24.6 billion (Centenaro et al., 2021), and more than 100 million users will have access to the satellite terminals. Therefore, the development of space-based IoT is facing the new technical challenge of how to meet the needs of massive user access under restricted spectrum resources.

Liu YJ et al. (2021) and Chen et al. (2022) proposed that in the context of spectrum resource constraints, increasing user access requires efficient and high-throughput multiple access techniques and improved utilization of limited spectrum resources. Currently, the commonly used multiple access techniques are frequency division multiple access (FDMA) (Deng et al., 2018), space division multiple access (SDMA) (Yao et al., 2018), time division multiple access (TDMA) (Vakil and Aghaeinia, 2009), code division multiple access (CDMA) (Wang X et al., 2022), and so on. Methods to improve spectrum utilization include cognitive radio technology (Zhang L et al., 2017), cellular multiplexing (Jabbari et al., 2010), and tapping into higher frequency bands, such as millimeter wave technology (Lei et al., 2023). Starlink, the second-generation system of SpaceX in the United States, achieves improved spectrum utilization by sharing the spectrum with other space-based and terrestrial users. Its new-generation satellite system communication bands are all Ku and Ka bands (Liu SJ et al., 2020). In addition, SpaceX is acquiring more spectrum resources through acquisitions and other means.

FDMA is a commonly used multiple access technique. Specifically, the FDMA technique works by dividing the channel frequency band into a number of narrower mutually exclusive sub-bands. Each subband is divided for the exclusive use of one user. When dividing the sub-frequency bands, it is necessary to leave a certain frequency-protection interval. This is done to avoid the neighboring channel interference due to the Doppler frequency offset (DFO) generated by the relative motion of the satellite and the ground terminal.

It is mentioned by Li ZJ (2023) that the DFO of a low-orbit satellite with an orbital altitude of 500 km would generate a frequency deviation of 12.6–142.2 kHz. Since the bandwidth and power resources of satellites are limited, leaving a certain frequency-protection interval to avoid neighboring channel interference would result in low bandwidth utilization to a certain extent. This results in output of fewer data, as well as fewer users being allowed to access the network.

Diao et al. (2012), Liu X et al. (2015), and Liu YQ et al. (2023) proposed to utilize the two-line orbital element (TLE) of the satellite message, combined with the orbital uptake model, to carry out orbital computation for any satellite with a known TLE message. Mao (2020) proposed a code-aided high-DFO calculation method with a low bit error rate. Wang C et al. (2017) proposed an algorithm for the joint estimation of the carrier frequency offset and carrier phase offset. Liu K and Zhu (2017) and Zhang JY et al. (2021) proposed methods to eliminate the Doppler frequency by adjusting the frame structure and through the leading sequence, respectively. However, the improvement in the number of users accessing the network is limited.

The effects of delay and DFO in star–ground links have been studied by Mao (2020), but the solutions given cannot flexibly adjust the subcarrier spacing according to the actual situation. DFO compensation has also been studied by Liu K and Zhu (2017) and Zhang JY et al. (2021), but the improvement in user access is limited. Dynamic fitting of DFO functions to predict and compensate for highly dynamic terminals has been proposed by Hou et al. (2015). However, realizing the real-time fitting of the function requires the real-time computation of the Greenwich mean time, which requires higher computational performance and energy consumption of the terminal. Yao et al. (2021), Yu A et al. (2023), and Yu TK et al. (2024b) proposed the use of edge computing and computing power networks to deal with large-scale resource scheduling problems to alleviate the central node computational pressure.

Inspired by the above literature, this paper proposes a spectrum resource utilization scheme based on DFO pre-compensation by using the idea of edge computing. It aims to address the high requirements for satellite performance in the way of DFO

compensation on the star when the satellite faces massive terminal access. Pre-compensation of the wide range of frequency deviations generated by the Doppler shift is carried out by means of a ground terminal. It achieves the purposes of reducing the frequency-protection interval, improving the spectrum utilization efficiency and the access volume of space-based IoT users, and avoiding real-time fitting calculations of the DFO function. This relieves the energy requirements and prolongs the service life of terminals, especially those located in areas that are off the beaten track, such as those in harsh geographical environments.

2 System model

2.1 Vector model of the relative position and relative velocity of a low-orbit satellite and a ground terminal

Using the simplified general perturbations 4 (SGP4) model, through the TLE of the satellite and the position of the ground terminal in longitude L, latitude B, and elevation H, as well as the motion state and direction of motion, the position and velocity vectors of the satellite and the ground terminal in the Earth-centered inertial (ECI) coordinate system can be obtained as $\boldsymbol{R}_{\rm sat}$, $\boldsymbol{V}_{\rm sat}$, $\boldsymbol{R}_{\rm g}$, and $\boldsymbol{V}_{\rm g}$, respectively. Thereafter, we use bold letters to represent vectors, and non-bold letters to represent scalars.

The relative position $\boldsymbol{r}$ and the relative velocity $\boldsymbol{v}$ of the satellite and the ground terminal are

$$\boldsymbol{r}=\boldsymbol{R}_{\rm sat}-\boldsymbol{R}_{\rm g}=\begin{bmatrix} r_x \\ r_y \\ r_z \end{bmatrix}, \boldsymbol{v}=\boldsymbol{V}_{\rm sat}-\boldsymbol{V}_{\rm g}=\begin{bmatrix} v_x \\ v_y \\ v_z \end{bmatrix}. \tag{1}$$

2.2 DFO model

Ground terminals and low Earth orbit (LEO) satellites will generate DFO due to relative motion during satellite communication. The relative motion between the LEO satellite and the various types of terminals is shown in Fig. 1.

According to the definition of Doppler shift, the DFO $f_{\rm Doppler}$ generated by the relative motion between the ground terminal and the satellite is shown in Eq. (2):

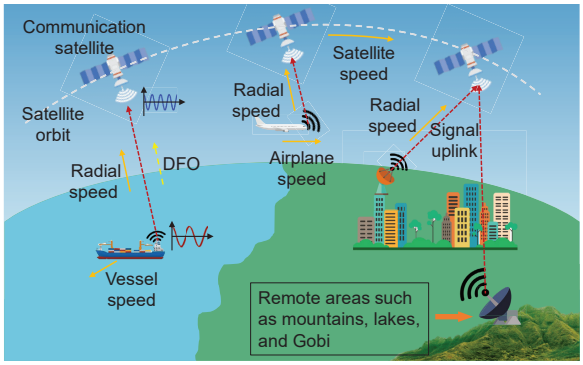

Fig. 1 Schematic diagram of the relative motion of the LEO satellite and various types of terminals

$$f_{\rm Doppler}=f_{\rm up}\cdot\frac{v}{c}\cdot\cos\beta, \tag{2}$$

where

$$\cos\beta=\frac{\boldsymbol{r}\cdot\boldsymbol{v}}{\|\boldsymbol{r}\|\cdot\|\boldsymbol{v}\|}, \beta\in(0,\pi), \tag{3}$$

$f_{\rm up}$ is the frequency of the signal sent from the ground terminal to the LEO satellite, v is the relative velocity between the ground terminal and the LEO satellite, c is the speed of light, and β is the angle between the signal transmission direction and the radial motion.

The frequency of the signal received at the receiving end on the star is shown in Eq. (4):

$$f=f_{\rm up}\pm f_{\rm Doppler}. \tag{4}$$

2.3 Channel segmentation model

Under a certain total bandwidth B_0, channel segmentation needs to take into account the channel bandwidth and isolation band required by the user. Among them, the channel bandwidth B_1 is related to the information transmission rate $R_{\rm s}$, the code rate $R_{\rm c}$, and the roll-off factor α:

$$B_1=\frac{R_{\rm s}(1+\alpha)}{R_{\rm c}}. \tag{5}$$

To prevent the DFO from interfering with neighboring channels, a protection interval $B_{\rm p}$ is required. Therefore, the required bandwidth B for a single user is

$$B=B_1+B_{\rm p}=B_1+2f_{\rm Doppler}. \tag{6}$$

The final number of channels that can be divided is

$$\text{Num}=\lfloor B_0/B\rfloor, \tag{7}$$

where $\lfloor\cdot\rfloor$ represents the rounding down operation.

3 Spectrum resource utilization technique based on DFO pre-compensation

The technical scheme proposed in this paper to improve the efficiency of spectrum resource utilization is shown in Fig. 2. First, the ground terminal calculates the relative motion parameters of the satellite and the ground terminal at the moment of message transmission through the TLE and SGP4 orbit model of the satellite. Then, according to the message length and transmission rate selected by the ground terminal, the number of message splits is judged and the value of DFO pre-compensation is computed. The transmitted signal is then compensated for using the optimal DFO compensation value. Next, the frequency-protection interval, which was originally set so large to prevent frequency interference due to DFO, is reduced. Finally, the channel resources are reallocated to accommodate more users and improve the spectrum utilization efficiency.

3.1 Determination of the Doppler frequency deviation protection interval

It is a continuous process for the ground terminal to send message signals to the receiving end of the LEO satellite. The duration is shown in Eq. (8). During the message-sending process, the relative position between the LEO satellite and the ground terminal is constantly changing. The DFO generated by the relative motion is also changing. Combined with Eqs. (2) and (3), its change rule can be expressed by Eq. (9).

$$T = \frac{N}{R_{\mathrm{s}}}, \tag{8}$$

$$\frac{\mathrm{d}f_{\mathrm{Doppler}}}{\mathrm{d}t} = \frac{f_{\mathrm{up}}}{c} \cdot \frac{\mathrm{d}(v\cos\beta)}{\mathrm{d}t} = \frac{f_{\mathrm{up}}}{c} \cdot \frac{\mathrm{d}v_{\mathrm{r}}}{\mathrm{d}t}, \tag{9}$$

where T is the message-sending duration, N is the message length, and v_{r} is the radial component of the relative velocity. Also, the relative motion between the satellite and the ground terminal is

$$r = \sqrt{R_{\mathrm{sat}}^2 + R_{\mathrm{g}}^2 - 2R_{\mathrm{sat}}R_{\mathrm{g}}\cos\alpha_{\mathrm{e}}}, \tag{10}$$

$$\begin{aligned} v_{\mathrm{r}} =& \frac{\mathrm{d}r}{\mathrm{d}t} \\ =& \frac{R_{\mathrm{sat}}R'_{\mathrm{sat}} + R_{\mathrm{g}}R'_{\mathrm{g}} - (R_{\mathrm{g}}R'_{\mathrm{sat}} + R_{\mathrm{sat}}R'_{\mathrm{g}})\cos\alpha_{\mathrm{e}}}{\sqrt{R_{\mathrm{sat}}^2 + R_{\mathrm{g}}^2 - 2R_{\mathrm{sat}}R_{\mathrm{g}}\cos\alpha_{\mathrm{e}}}} \\ & - \frac{R_{\mathrm{sat}}R_{\mathrm{g}}\frac{\mathrm{d}\cos\alpha_{\mathrm{e}}}{\mathrm{d}t}}{\sqrt{R_{\mathrm{sat}}^2 + R_{\mathrm{g}}^2 - 2R_{\mathrm{sat}}R_{\mathrm{g}}\cos\alpha_{\mathrm{e}}}}, \end{aligned} \tag{11}$$

where α_{e} is the angle between the ground terminal and the satellite about the center of the Earth, due to the fact that the orbital altitude of the LEO satellite is <2000 km, and $\alpha_{\mathrm{e\,max}} = \arccos\left(\frac{R_{\mathrm{E}}}{R_{\mathrm{sat}}}\right) = 0.7058\,\mathrm{rad}$ (R_{E} is the radius of the Earth). $R_{\mathrm{sat}} = \|\boldsymbol{R}_{\mathrm{sat}}\|$, $R_{\mathrm{g}} = \|\boldsymbol{R}_{\mathrm{g}}\|$, and R'_{sat} (R'_{g}) represents the first derivative of position with respect to time. Also, the message-sending duration T is much smaller than the orbital period, so the effect of the Earth's rotation can be ignored, and the distance between the satellite and the ground terminal from the center of

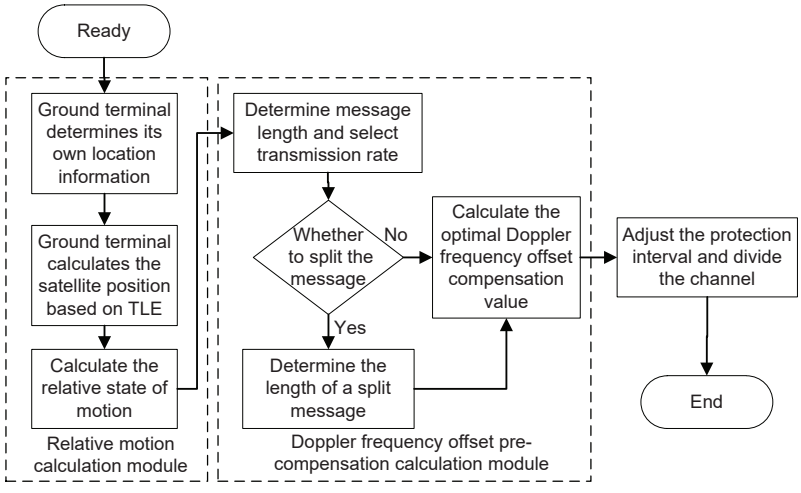

Fig. 2 Spectrum resource utilization scheme based on DFO pre-compensation

the Earth can be approximated as constant. Thus, Eq. (11) can be simplified as

$$v_{\mathrm{r}}=-\frac{R_{\mathrm{sat}}R_{\mathrm{g}}}{r}\frac{\mathrm{d}\cos\alpha_{\mathrm{e}}}{\mathrm{d}t}=\frac{R_{\mathrm{sat}}R_{\mathrm{g}}\sin\alpha_{\mathrm{e}}}{r}\frac{\mathrm{d}\alpha_{\mathrm{e}}}{\mathrm{d}t}, \quad (12)$$

$$\begin{aligned}\frac{\mathrm{d}v_{\mathrm{r}}}{\mathrm{d}t}=&\frac{R_{\mathrm{sat}}R_{\mathrm{g}}}{r}\left(\cos\alpha_{\mathrm{e}}\left(\frac{\mathrm{d}\alpha_{\mathrm{e}}}{\mathrm{d}t}\right)^2+\sin\alpha_{\mathrm{e}}\frac{\mathrm{d}^2\alpha_{\mathrm{e}}}{\mathrm{d}t^2}\right)\\&-\frac{R_{\mathrm{sat}}^2R_{\mathrm{g}}^2}{r^3}\left(\sin^2\alpha_{\mathrm{e}}\left(\frac{\mathrm{d}\alpha_{\mathrm{e}}}{\mathrm{d}t}\right)^2\right).\end{aligned} \quad (13)$$

Since the orbits of LEO communication satellites are predominantly near-circular in design, and according to the relationship between the three sides of an obtuse triangle, it is easy to obtain $r^2\cos\alpha_{\mathrm{e}}\geq R_{\mathrm{sat}}R_{\mathrm{g}}\sin^2\alpha_{\mathrm{e}}$, $\alpha_{\mathrm{e}}\leq\alpha_{\mathrm{e\,max}}$. Thus, the change in f_{Doppler} is related to α_{e}. The process of α_{e} decreasing to 0 and then increasing corresponds to the process of the satellite moving closer to and then farther away from the terminal, and f_{Doppler} changes accordingly with r.

Therefore, the frequency-protection interval needs to consider the DFO changes during the whole message transmission. As shown in Fig. 3, it is the ideal case that the DFO is fully compensated for. The signal frequency received by the receiver on the star has no DFO. There is no need to set additional protection intervals, and the frequency resources can be fully utilized for channel segmentation.

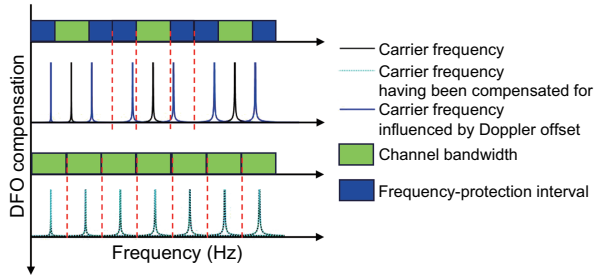

Fig. 3 Protection interval setting after DFO compensation in the ideal case

In practice, the full realization of DFO pre-compensation requires real-time calculation and adjustment of the compensation value for the whole transmitting process. This imposes significant power consumption and high computational requirements on the transmitting terminal, while placing stringent technical demands on the ground terminal equipment. However, without DFO pre-compensation, the large protection interval greatly reduces the efficiency of frequency resource utilization. Comprehensively considering the performance conditions of the terminal equipment, we propose one-time computation with continuous compensation to reduce the DFO protection interval.

The ground terminal calculates the time period covered by the LEO satellite beam. Then the DFO $f_{\mathrm{Doppler},1}$ and $f_{\mathrm{Doppler},2}$ generated by the uplink of the signal frequency at the start moment t_1 and the end moment t_2 of the ground terminal being covered and the applied DFO compensation value f_{c} are calculated. Then the protection interval Δf of the DFO is set as shown in Eq. (14):

$$\Delta f=\max\left(\left|f_{\mathrm{c}}-f_{\mathrm{Doppler},1}\right|,\left|f_{\mathrm{c}}-f_{\mathrm{Doppler},2}\right|\right). \quad (14)$$

3.2 Determination of the optimal compensation frequency for Doppler frequency deviation

The DFO protection interval is changed when the moment of choosing to calculate the DFO is different. Through research and analysis, the DFO of the LEO satellite has the same change rule in the two motion processes of approaching and moving away from the ground terminal. The process of the LEO satellite moving away from the ground terminal is selected to determine the optimal pre-compensation frequency of DFO.

The DFO pre-compensation value can be calculated by selecting the start moment t_1, middle moment t_0, and end moment t_2 of the message, $t_1<t_0<t_2$, $r_1<r_0<r_2$. From Eqs. (9) and (12), DFO is increasing during message transmission:

$$f_{\mathrm{Doppler},1}\leq f_{\mathrm{Doppler}}\leq f_{\mathrm{Doppler},2}. \quad (15)$$

Without DFO pre-compensation, the required bandwidth range to avoid mutual interference between the channels is $[f_{\mathrm{up}}-f_{\mathrm{Doppler},2},f_{\mathrm{up}}+f_{\mathrm{Doppler},2}]$. The DFO protection interval is set to $\Delta f=\max(f_{\mathrm{Doppler}})=f_{\mathrm{Doppler},2}$. The DFO compensation value f_{c} that can be applied is

$$0\leq f_{\mathrm{c}}\leq f_{\mathrm{Doppler},2}. \quad (16)$$

Overcompensation can also lead to channel interference when $f_{\mathrm{Doppler}}<f_{\mathrm{c}}$. An additional protection interval $\Delta f'=f_{\mathrm{c}}-f_{\mathrm{Doppler}}$ is required. Therefore, the DFO protection interval Δf needs to satisfy

Eq. (17) when $t_1 \le t \le t_2$:

$$f_{\mathrm{up}} + f_{\mathrm{c}} + \Delta f = f_{\mathrm{up}} + f_{\mathrm{Doppler}}(t). \tag{17}$$

Substituting inequalities (15) and (16) into Eq. (17) yields

$$\frac{f_{\mathrm{Doppler},2} - f_{\mathrm{Doppler},1}}{2} \le \Delta f \le f_{\mathrm{Doppler},2}. \tag{18}$$

To obtain as many new channels as possible, $\sum_{t_1 \le t \le t_2} |f_{\mathrm{Doppler}}(t) - f_{\mathrm{c}}|$ needs to be minimized. The protection interval $\Delta f_{\min} = \frac{f_{\mathrm{Doppler},2} - f_{\mathrm{Doppler},1}}{2}$ needs to be set when $f_{\mathrm{c}} = \frac{f_{\mathrm{Doppler},2} + f_{\mathrm{Doppler},1}}{2}$. This is the optimal compensation frequency for DFO:

$$f_{\mathrm{c,best}} = \frac{f_{\mathrm{Doppler},2} + f_{\mathrm{Doppler},1}}{2}. \tag{19}$$

3.3 Determination of the number of message splits

As shown in Eqs. (9) and (13), the DFO generated by the relative motion between the LEO satellite and the ground terminal is affected mainly by the satellite's orbital characteristics, and it changes continuously with time. Therefore, the effect of the message transmission time, which is determined mainly by the message length and transmission rate, needs to be considered in the DFO pre-compensation.

When the transmission rate is certain and the length of the message sent by the terrestrial terminal is short, the purpose of improving spectrum utilization efficiency can be achieved without splitting the message. However, when the length of the message sent by the terminal is long, it is still necessary to set a large DFO protection interval with single DFO calculation and compensation.

Therefore, we set the transmission time threshold $\tau = T/n$, and the accuracy thresholds ε and n for the number of message splits satisfy

$$\tau_n - \tau_{n+1} < \varepsilon. \tag{20}$$

As shown in Fig. 4, when $T > \tau$, the original long message is split into several short messages. The number of split short messages is continuously adjusted to make it meet the requirements of $T_1, T_2, \ldots, T_n \le \tau$.

Select appropriate DFO values to compensate for the split short messages in turn according to inequalities (16) and (18), and the new protection interval Δf after splitting should satisfy Eq. (21):

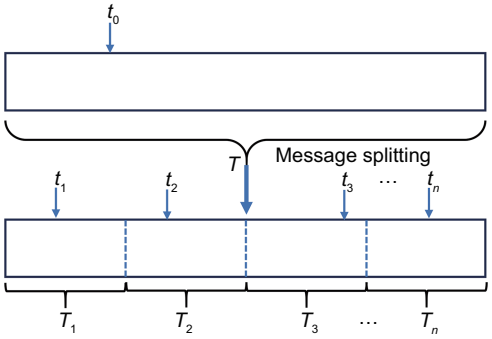

Fig. 4 Schematic diagram of splitting a long message into multiple short messages

$$\Delta f = \max\left(\left|f_{\mathrm{Doppler},i_1} - f_{\mathrm{c},i}\right|, \left|f_{\mathrm{c},i} - f_{\mathrm{Doppler},i_2}\right|\right), \quad i = 1, 2, \ldots, n, \tag{21}$$

where $f_{\mathrm{c},i}$ is the DFO pre-compensation value for the i^{th} short message.

However, more splits do not always mean better performance. While considering the reduction of the protection interval, it is also important to consider the computational complexity. To avoid the resource loss caused by excessive message splitting, the splitting measure is set. The time complexity of the proposed method is

$$O(n) = T/\varepsilon \cdot O(1). \tag{22}$$

It means that the optimal number of message splits changes with the different ε settings.

4 Simulation and analysis

4.1 Parameter configuration

A ground-fixed sensor, a low-speed moving vessel, and a civil aviation airplane in a high-speed cruising state are selected as ground terminals. The simulation parameters are shown in Table 1.

Table 1 Distribution of ground terminals

Terminal type	Longitude (°)	Latitude (°)	Elevation (m)	Velocity (m/s)
Ground-fixed sensor	112.3840	26.7147	68.5453	0
Low-speed vessel	123.8612	30.0570	0	15.4333
Civil aviation airplane	123.8900	30.4321	10 668	250

An LEO satellite with normal operation in orbit is selected as the satellite receiving end. The maximum angle of the satellite antenna beam is set to 60°. The TLE message parameters of the LEO satellite are shown in Table 2.

According to the simulation needs, three different message lengths of 25, 50, and 100 bytes, as well as four different information transmission rates of 1024, 512, 256, and 128 bit/s are set. The quadrature phase shift keying (QPSK) modulation is used. The roll-off factor $\alpha = 0.5$ is set, and the signal is transmitted at a frequency of 12 GHz with a bandwidth of 10 MHz.

4.2 Comparison of the effect of pre-compensation on the improvement of subscriber access

First, the DFO patterns of three different types of terminals are compared and analyzed, as shown in Fig. 5. It can be seen that the different deployments of terminal positions and different moving speeds only have an impact on the resulting DFO value. However, the change rule of DFO is the same. Therefore, for the convenience of the research, a fixed terminal is selected in the following for the comparison of the effect of DFO pre-compensation on the improvement of the number of access users.

4.2.1 Effect of the same message length at different transmission rates

The ground terminal is simulated to send messages of 25 bytes in length at randomly selected times at four information transmission rates of 128, 256, 512, and 1024 bit/s. We compare the number of users accessed in the case of no compensation, pre-compensation for DFO, and ideal no-DFO, and the number of users that can be accessed more by reclassifying the channel with idle frequency after performing compensation. The results are shown in Fig. 6.

The simulations show that while transmitting the 25-byte short message at 128, 256, 512, and 1024 bit/s codeword rates, the number of access users can be increased by up to 4036, 6525, 7430, and 5481, respectively, by performing DFO calculations once and compensating. By means of DFO pre-compensation, the frequency originally used as a protection interval is released and used to be divided into channels, thereby the number of access users after compensation has been substantially increased by about 252, 407, 464, and 342 times compared with that without compensation. Also, the optimal compensation value determined by using Eq. (19) allows the access user quantity to increase by 48% compared to the general method.

Meanwhile, as the information transmission rate increases, the number of users accessed after pre-compensation gradually converges to the number of

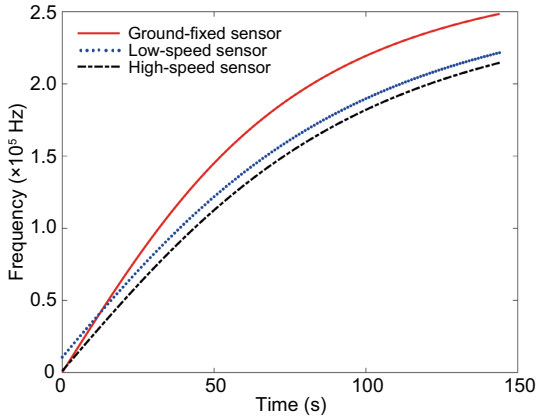

Fig. 5 DFO over time for different terminal types

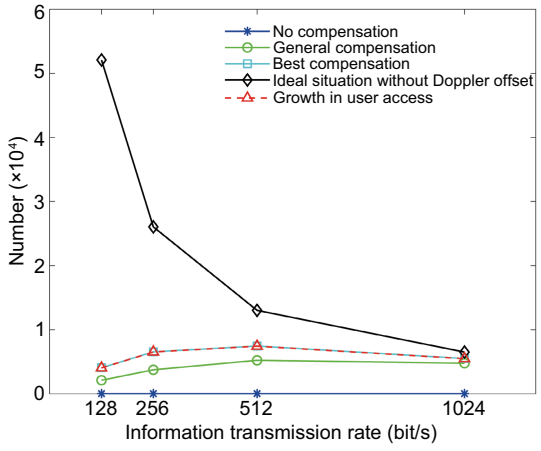

Fig. 6 Variation in the number of DFO pre-compensated access users at different information transmission rates

Table 2 Starlink-1007 satellite ephemeris

1	44713U	19074A	23 303.808 664 86	0.000 024 95	00000+0	18641-3	0	9999
2	44713	53.0535	91.2629	0001292	85.1075	275.0062	1215.063 818 312 191 68	

users accessed under the ideal no-DFO. This is due to the fact that the signal bandwidth is positively correlated with the transmission rate of the symbol elements. After DFO pre-compensation, the frequency band originally allocated as protection intervals can be repurposed for channel partitioning. Lower transmission rates require fewer spectral resources, enabling the allocation of additional channels.

However, for the case of a smaller information transmission rate, more time is required to transmit the same length of message. The DFO generated by the relative motion between the LEO satellite and the terminal during transmission is also changing with time. This results in a larger DFO even after pre-compensation. It is still necessary to set a large protection interval to protect the neighboring frequencies from interference with each other. So, it has led to a decrease in the number of new subscribers. Therefore, the higher the information transmission rate, the shorter the transmission time and the less the DFO is affected by the relative motion. The closer the compensated increase in the number of access users is to the ideal situation, the better the result is.

4.2.2 Effect of the same transmission rate at different message lengths

DFO pre-compensation is also performed for the same transmission rate at three different message lengths (25, 50, and 100 bytes), and the increase in the number of access users is obtained, as shown in Fig. 7.

Comparative analysis reveals that the shorter the message, the larger the increment in the number of users after DFO pre-compensation at the same codeword rate. Their average access user numbers increase by about 225, 152, and 98 times, respectively. It can be concluded that the method of pre-compensation by calculating the DFO value at one time for terrestrial terminals is better than that for long messages to enhance the effect of short messages.

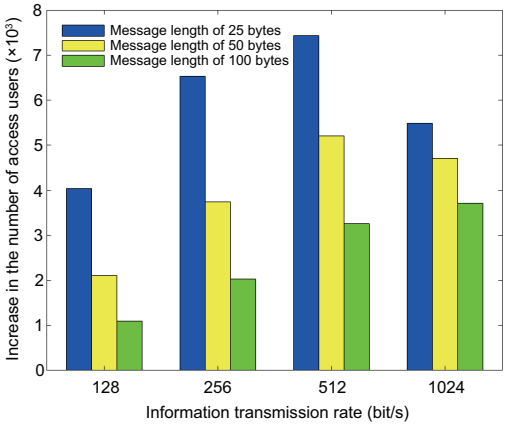

Fig. 7 DFO pre-compensated access user number increment for different message lengths

It is also found that at a certain transmission rate, the effect of DFO pre-compensation on increasing the number of access users increases as the rate increases. However, when the short message is sent at 512 and 1024 bit/s, the increase of the user number has a decreasing trend. This is because the bandwidth required for message transmission is related to the symbol element transmission rate as shown in Eq. (5). When transmitting a 25-byte message at an information transmission rate of 512 or 1024 bit/s, the pre-compensated frequency-protection interval is set to 286.54 or 139.83 Hz, respectively. The bandwidths required for transmitting a short message are 768 and 1536 Hz, respectively. The signaling bandwidths increase with the increase of the information transmission rate, resulting in the reduction of the number of channels to be divided. This in turn leads to a decrease in the number of users that can be added by DFO pre-compensation. Therefore, the chosen information transmission rate is not as large as possible.

4.2.3 Compensation effect for the number of long message splits

To further improve the spectrum utilization efficiency, it is necessary to compensate for the significant gap between actual and ideal user access capacity growth caused by excessive packet length and prolonged transmission time. The scheme of splitting the message is proposed for the message whose transmission time is too long. The message with long transmission time is split into several short messages. Also, the DFO is calculated for each short message and pre-compensated for separately. This method of message splitting can be used on messages of different lengths and transmission rates.

In this experiment, a 100-byte message transmitted at 128 bit/s, which is most affected by the transmission time, is selected for research and analysis. $\varepsilon = 0.005$ is set. The optimal DFO compensation

value is obtained according to Eq. (19) and the protection interval is set with Eq. (21). The simulation results are shown in Fig. 8.

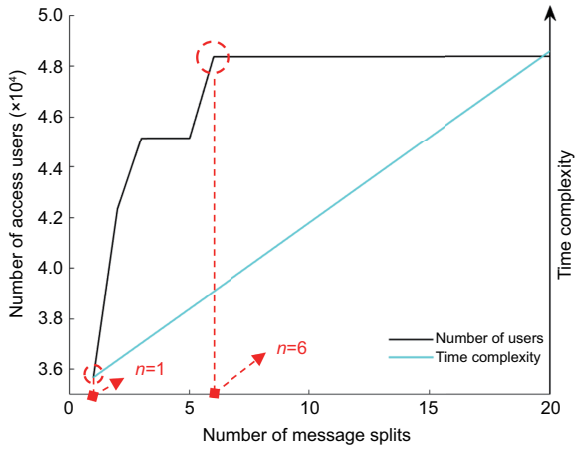

Fig. 8 Relationship between the number of message splits and the number of access users and time complexity

Therefore, splitting a 100-byte message transmitted at 128 bit/s into six segments and calculating the DFO pre-compensation value for each segment provides the best compensation effect. The number of access users increases by about 35.6% compared to the unsplit message with a corresponding length and transmission rate. It can be seen that splitting the message several times does help increase the number of access users and has less impact on the time complexity.

Finally, we compare the time complexity of three DFO compensation approaches under increasing message transmission durations: satellite-centralized DFO compensation, ground terminal real-time Doppler function fitting with pre-compensation, and the DFO pre-compensation scheme proposed in the paper.

From Fig. 9, it can be seen that if edge computing is not adopted, the time complexity of the operation on the satellite will increase with the increase in the number of access users. As for the terrestrial terminal, if the real-time prediction of DFO is used for compensation, its time complexity will increase with the growth of message transmission time. However, the compensation method proposed in this paper does not need to predict the DFO in the whole process. Instead, the number of message splits that should be performed at the corresponding transmission rate and message length can be set for the terminal in advance. Then the DFO at the corresponding moment is predicted, which greatly reduces the computation. Also, it can be seen from Fig. 6 that the gap between the number of users after pre-compensation and the number of users in the ideal state gradually decreases with the increase of the information transmission rate. Meanwhile, the time complexity is related to the computation. The smaller computation of this method reduces the energy consumption of the ground terminal, and the service life of the terminal located in unfavorable environments is extended.

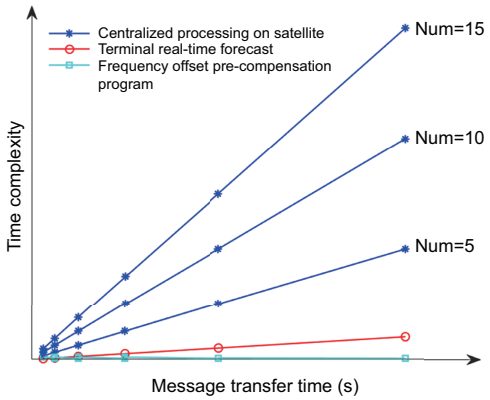

Fig. 9 Variation of time complexity with transmission time for the three methods

5 Conclusions

In this paper, a spectrum utilization scheme based on DFO pre-compensation is proposed to address the need to set a large protection interval for preventing frequency interference caused by the DFO, which is generated by the relative motion between LEO satellites and ground terminals. This technical scheme utilizes edge computing. First, the ground terminal extrapolates the relative motion between the LEO satellite and the ground terminal based on the TLE message. Then, according to the actual needs of the mission, the appropriate message length and transmission rate are selected. Thereafter, the number of times a message needs to be split and the optimal DFO pre-compensation value are determined. Finally, the frequency-protection interval is readjusted and new channels are divided. Three message lengths and four information transmission rates that can be used in combination with

each other are given, which can increase the number of users accessing the network by up to about 400 times. The efficiency of spectrum resource utilization is greatly improved. This provides a scheme to better solve the problem of terrestrial extremely massive user access.

Compared with the real-time fitting of the DFO function, this scheme makes the required computation volume smaller and the computation time requirement lower by sacrificing part of the channel resources. It extends the service life of ground terminals in remote areas and better meets the needs of space-based IoT user terminals in remote and harsh environments. However, this scheme will greatly rely on the TLE data from the satellite, and the TLE data stored in the terminal need to be updated periodically.

Contributors

Qingquan LIU and Lihu CHEN designed the research. Qingquan LIU processed the data and drafted the paper. Songting LI, Yiran XIANG, and Baokang ZHAO helped organize the paper. Qingquan LIU, Lihu CHEN, and Baokang ZHAO revised and finalized the paper.

Conflict of interest

All the authors declare that they have no conflict of interest.

Data availability

The data that support the findings of this study are available from the corresponding author upon reasonable request.

References

Centenaro M, Costa CE, Granelli F, et al., 2021. A survey on technologies, standards and open challenges in satellite IoT. *IEEE Commun Surv Tut*, 23(3):1693-1720. https://doi.org/10.1109/COMST.2021.3078433

Chen LH, Cui JW, Li ST, 2022. Key technologies and application prospects for space-based Internet of Things. *Space Int*, 2022(1):26-32 (in Chinese).

Deng QY, Li ZT, Chen JB, et al., 2018. Dynamic spectrum sharing for hybrid access in OFDMA-based cognitive femtocell networks. *IEEE Trans Veh Technol*, 67(11):10830-10840. https://doi.org/10.1109/TVT.2018.2869755

Diao NH, Liu JQ, Sun CR, et al., 2012. Satellite orbit calculation based on SGP4 model. *Remote Sens Inform*, 27(4):64-70 (in Chinese). https://doi.org/10.3969/j.issn.1000-3177.2012.04.011

FCC, 2002. Spectrum Policy Task Force. Technical Report, ET Docket No. 02-135. Federal Communications Commission, USA.

Ge LJ, Li Y, Tao J, 2016. Time and frequency synchronization scheme for IEEE802.15.3c OFDM system. *J Commun*, 11(2):143-148. https://doi.org/10.12720/jcm.11.2.143-148

Hou HL, Chen YJ, Ding S, et al., 2015. Estimation and compensation method for the Doppler frequency shift of high dynamic terminal in LEO satellite communication system. *J Comput Inform Syst*, 11(15):5717-5728.

Jabbari B, Pickholtz R, Norton M, 2010. Dynamic spectrum access and management. *IEEE Wirel Commun*, 17(4):6-15. https://doi.org/10.1109/MWC.2010.5547916

Lei HJ, Zhou S, Park KH, et al., 2023. Outage analysis of millimeter wave RSMA systems. *IEEE Trans Green Commun*, 71(3):1504-1520. https://doi.org/10.1109/TCOMM.2023.3235349

Li K, Li F, Yang WM, 2023. Space-based Internet of Things: basic concepts, system architecture and development trends. *Telecommun Eng*, 63(2):281-290 (in Chinese). https://doi.org/10.20079/j.issn.1001-893x.211207003

Li ZJ, 2023. Design of low Earth orbit space-based Internet of Things systems. *Mob Commun*, 47(7):98-103 (in Chinese). https://doi.org/10.3969/j.issn.1006-1010.20230214-0001

Liu K, Zhu LD, 2017. Research on the random access technology of LTE based satellite mobile communications. *Radio Commun Technol*, 43(2):12-15 (in Chinese). https://doi.org/10.3969/j.iss.1003-3114.2017-02.03

Liu SJ, Xu FJ, Liu LY, et al., 2020. Introduction of Starlink second generation system. *Satell Netw*, 12:62-65 (in Chinese).

Liu X, Huang C, Cui YQ, et al., 2015. Research on Doppler frequency-shift compensation method based on SGP4 model in satellite communication systems. *Sci Technol Eng*, 15(21):154-158 (in Chinese). https://doi.org/10.3969/j.issn.1671-1815.2015.21.030

Liu YJ, Li BC, Wang YZ, 2021. Key issues in development and application of the sky-based Internet of Things. *Space Integr Ground Inform Netw*, 2(1):81-86 (in Chinese). https://doi.org/10.11959/j.issn.2096-8930.2021011

Liu YQ, Li HG, Shi JL, et al., 2023. Doppler frequency offset pre-compensation algorithm based on mixed forcast for LEO satellite communications. *Chin High Technol Lett*, 33(6):559-567 (in Chinese). https://doi.org/10.3772/j.issn.1002-0470.2023.06.001

Mao X, 2020. Research on Synchronization and Access Technologies for Satellite OFDM Systems. MS Thesis, National Key Laboratory of Science and Technology on Communications, Chengdu, China (in Chinese). https://doi.org/10.27005/d.cnki.gdzku.2020.001565

Tan X, Wang H, Fu LZ, et al., 2018. Collision detection and signal recovery for UHF RFID systems. *IEEE Trans Autom Sci Eng*, 15(1):239-250. https://doi.org/10.1109/TASE.2016.2614134

Vakil V, Aghaeinia H, 2009. Throughput analysis of STS-based CDMA system with variable spreading factor in non-frequency selective Rayleigh fading channel. *Comput Electr Eng*, 35(4):528-535. https://doi.org/10.1016/j.compeleceng.2008.08.001

Wang C, Cui GF, Wang WD, et al., 2017. Joint estimation of carrier frequency and phase offset based on pilot symbols in quasi-constant envelope OFDM satellite systems. *China Commun*, 14(7):184-194. https://doi.org/10.1109/CC.2017.8019135

Wang X, Chen HH, Liu XQ, et al., 2022. Complementary coded CDMA with multi-layer quadrature modulation. *IEEE Trans Veh Technol*, 71(3):2991-3007. https://doi.org/10.1109/TVT.2022.3142939

Yang H, Yuan JQ, Li C, et al., 2022. BrainIoT: brain-like productive services provisioning with federated learning in industrial IoT. *IEEE Int Things J*, 9(3):2014-2024. https://doi.org/10.1109/JIOT.2021.3089334

Yang Y, 2019. Research on Decision-Making Mechanism for Improving Adaptability of Cognitive Radio. PhD Dissertation, Harbin Institute of Technology, Shenzhen, China (in Chinese).

Yao QY, Yang H, Zhu RJ, et al., 2018. Core, mode, and spectrum assignment based on machine learning in space division multiplexing elastic optical networks. *IEEE Access*, 6:15898-15907. https://doi.org/10.1109/ACCESS.2018.2811724

Yao QY, Yang H, Bao BW, et al., 2021. Federated transfer learning-based data security assurance in edge optical networks for IoT applications. Proc Asia Communications and Photonics Conf, p.1-3.

Yu A, Yang H, Feng CY, et al., 2023. Socially-aware traffic scheduling for edge-assisted metaverse by deep reinforcement learning. *IEEE Netw*, 37(6):74-81. https://doi.org/10.1109/MNET.2023.3317108

Yu TK, Yang H, Nie JL, et al., 2024a. Bias-compensation augmentation learning for semantic segmentation in UAV networks. *IEEE Int Things J*, 11(12):21261-21273. https://doi.org/10.1109/JIOT.2024.3373454

Yu TK, Yang H, Yao QY, et al., 2024b. Multi-visual-GRU-based survivable computing power scheduling in metro optical networks. *IEEE Trans Netw Serv Manag*, 21(1):1302-1315. https://doi.org/10.1109/TNSM.2023.3314272

Zhang JY, Yu ZY, Zhu M, et al., 2021. Design of carrier synchronization algorithm for SCMA system in LEO satellite communication. *Syst Eng Electron*, 43(5):1354-1360 (in Chinese). https://doi.org/10.12305/j.issn.1001-506X.2021.05.24

Zhang L, Xiao M, Wu G, et al., 2017. A survey of advanced techniques for spectrum sharing in 5G networks. *IEEE Wirel Commun*, 24(5):44-51. https://doi.org/10.1109/MWC.2017.1700069